

Indirect detection of a subdominant density component of cold dark matter

Gintaras Duda, Graciela Gelmini
Department of Physics and Astronomy, UCLA
Los Angeles, CA 90095-1547, USA
gkduda, gelmini@physics.ucla.edu

Paolo Gondolo
Department of Physics, Case Western Reserve University
10900 Euclid Ave., Cleveland, OH 44106-7079, USA
pxg26@po.cwru.edu

Joakim Edsjö
Department of Physics, Stockholm University
AlbaNova, SE-106 91, Stockholm, Sweden
edsjo@physto.se

Joseph Silk
Department of Physics, University of Oxford
Denys Wilkinson Building, Keble Road, Oxford OX1 3RH, UK
silk@astro.ox.ac.uk

Abstract

We examine the detectability through indirect means of weakly interacting dark matter candidates that may constitute not all but only a subdominant component of galactic cold dark matter. We show that the possibility of indirect detection of neutralinos from their annihilations in the Earth and Sun is not severely hampered by decreasing neutralino relic density. Upward-going muon fluxes in underground detectors from neutralino annihilations in the Sun can remain above the threshold of detectability of 10 muons/km²/yr for neutralinos composing 1% or more of the halo dark matter. Similarly, signals from neutralino annihilations in the Earth can also remain high for neutralino densities of 1% of the halo and actually would only be observable close to this low density for neutralinos lighter than 150 GeV. We also show that there are many models which simultaneously have high direct and indirect detection rates making some model discrimination possible if a signal is seen in any of the current dark matter searches.

We examine the observability of collisionless cold dark matter (CCDM) by indirect detection when it is merely a subdominant component of the cold dark matter. Originally we were led to consider such a question by claims of the need for collisional cold dark matter [1] as the main form of dark matter in the universe, but the question is valid independently of such claims. Even if non-CCDM is proven to be unnecessary, there remains the possibility of the CDM consisting of several populations, the one we are searching for not being the dominant one. So the question is: if the previously favored CDM candidates, such as Weakly Interacting Massive Particles (WIMPs), constitute only a fraction, say 1% or less, of the local dark matter halo, would these particles still be observable in the current and proposed direct and indirect dark matter searches? We could even reverse our question in the following manner: if we see a CDM signal in any of our searches, could we be observing a subdominant component of the total CDM? Additionally, could a combination of direct and indirect detection data resolve the issue of which component of the total CDM we are observing?

Unless there is segregation for different types of cold dark matter, the ratio of collisionless CDM to total CDM should be the same locally in the Galaxy and globally in the whole Universe. This is expected if all CDM components are collisionless. Thus in the following we assume that the local fraction of the particular collisionless CDM f_{CCDM} is related to the CCDM density parameter Ω_{CCDM} (the CCDM relic density in units of the critical density) through

$$f_{CCDM} = \frac{\rho_{CCDM}}{\rho_{\text{local}}} = \frac{\Omega_{CCDM}}{\Omega_{CDM}}. \quad (1)$$

Here ρ_{CCDM} is the local density of a particular CCDM candidate, such as a particular WIMP, $\rho_{\text{local}} \simeq 0.3 \text{ GeV}/\text{cm}^3$ is the local halo density (at the location of the Earth), Ω_{CCDM} is the relic density of our particular CCDM candidate, and $\Omega_{CDM} \simeq 0.3$ is the total contribution of DM to the total energy density of the Universe.

Naively, one may expect that if the local CCDM density is, say, $f_{CCDM} = 1\%$ of the local halo density, the fluxes of particles produced by WIMP-WIMP annihilations in the halo and elsewhere, being proportional to some power n of the local WIMP density, would decrease by an amount f_{CCDM}^n , i.e. by 0.01^n in our example. However, the relic density of thermal WIMPs Ω_χ is approximately determined by their annihilation cross-section σ_a through the relation

$$\Omega_\chi h^2 \simeq \frac{3 \times 10^{-27} \text{ cm}^3/\text{sec}}{\langle \sigma_a v \rangle_{E.U.}}, \quad (2)$$

where $\langle \sigma_a v \rangle_{E.U.}$ is the thermal average of the annihilation cross section times the relative velocity of the WIMPs at freeze-out, in the early universe, and h is the reduced Hubble constant, $h \simeq 0.7$. Hence a reduction in the relic WIMP density requires an increase in their annihilation cross-section in the early Universe. In

general, $\langle\sigma_a v\rangle_{E.U.}$ is related to $\langle\sigma_a v\rangle$, the annihilation cross section of WIMPs in the galactic halo or at the center of the Sun or of the Earth. These two averaged annihilation cross sections differ in the temperature of the WIMPs when they annihilate: about a twentieth of the WIMP mass in the early universe, practically zero in the halo, the Sun and the Earth. However, there are exceptions to this relation: when coannihilations [2] are important the WIMP population has to be followed together with the population of other particles with which it can be interchanged. As a consequence, $\langle\sigma_a v\rangle_{E.U.}$ is an effective annihilation quantity that includes annihilation of and with other particles, and which is not directly related to $\langle\sigma_a v\rangle$ at zero temperature. Since the annihilation signals are in general proportional to the product of the annihilation cross section and the *square* of the WIMP density, and the latter decreases linearly with the annihilation cross section, a more educated statement is that the annihilation signals decrease linearly with WIMP density. This is the case if $\langle\sigma_a v\rangle_{E.U.}$ and $\langle\sigma_a v\rangle$ are proportional. We will see below (Fig. 3) that this linear decrease is true for the envelope of the largest signals of neutralino annihilation in the halo.

The situation is more complicated when the signals depend not only on the annihilation cross section σ_a , but also on the scattering cross section σ_s of WIMPs with nucleons. Besides direct detection, this is important for WIMP annihilation in the Sun and the Earth. The number of WIMPs accumulated in those bodies is proportional to $\sigma_s \rho_{CCDM}$, i.e. to $\sigma_s \sigma_a^{-1}$. So at short times the annihilation signal goes as $\sigma_a (\sigma_s \sigma_a^{-1})^2$. At times much longer than the equilibration time between WIMP capture and annihilation, instead, the annihilation signal depends entirely on the product $\sigma_s \rho_{CCDM} \sim \sigma_s \sigma_a^{-1}$, since in equilibrium the annihilation rate equals the capture rate.

Now, the scattering cross section is not independent of the annihilation cross section. As argued in earlier papers [3, 4, 5], when the annihilation cross section grows, the scattering cross section may grow by the same factor. If so, the product $\sigma_s \rho_{CCDM} \sim \sigma_s \sigma_a^{-1}$ remains approximately constant, and signals proportional to this product, such as those from equilibrium annihilation in the Sun and Earth, remain nearly unchanged.

Scattering and annihilation cross sections of WIMPs are in general related by a crossing symmetry. Unpolarized cross sections are spin sums of amplitudes squared, and a crossing symmetry relates the amplitudes of two processes that differ by having a particle in the final state exchanged with a particle in the initial state, both becoming their respective antiparticle. For example, the amplitude for neutralino-quark scattering $\chi q \rightarrow \chi q$ is related to the amplitude for neutralino-neutralino annihilation into quark-antiquark pairs $\chi\chi \rightarrow q\bar{q}$. Often, other annihilation channels besides $q\bar{q}$ are open, such as annihilation into W or Z boson pairs, and since these particles are not present in the nucleon, the crossing symmetry is imperfect. Moreover, the scattering and annihilation cross sections are computed at different kinematical points, and may differ in the spin structure, the presence of resonances, the integration limits over momenta, etc.

The relation between the WIMP annihilation cross section and the cross

section for WIMP scattering off nucleons is further complicated by the fact that annihilation can be considered to produce quark-antiquark pairs, while scattering occurs with quarks bound in nucleons. The annihilation amplitudes are functions of the quark masses, while the scattering amplitudes are functions of the nucleon mass. Moreover, the scattering amplitude contains the matrix elements of the quark currents in the nucleon, which are of course not present in the annihilation amplitude into quark-antiquark pairs.

Despite these imperfections in the crossing symmetry, we can see it at work in the case where WIMPs are neutralinos in the Minimal Supersymmetric Standard Model (MSSM), with some sets of parameters. We use the version of the MSSM described in [6], whose seven input parameters are given at the weak scale, as implemented in the DarkSUSY code [7]. In Fig. 1 we make the crossing symmetry explicit in a particular example.

We present a set of models obtained by modifying only the neutralino composition (and thus its couplings) starting from a single original model that exhibits high muon fluxes from neutralino annihilations in the Earth at low neutralino relic density (we argue later that this high flux is due directly to the compensation provided by the crossing symmetry). The particular parameter values of the original model (one of the points in Fig. 1) are as follows: the mass of the neutralino $m_\chi = 147.9$ GeV, the mass of the CP-odd Higgs boson $m_A = 113.1$ GeV, the ratio of Higgs vacuum expectation values $\tan\beta = 47.52$, the sfermion mass parameter $m_0 = 1873$ GeV, and the trilinear couplings in the top and bottom sectors $A_t = -1.758m_0$ and $A_b = -2.152m_0$. This particular original model has a neutralino relic density of $\Omega_\chi h^2 = 2.9 \times 10^{-3}$, a neutralino gaugino fraction $Z_g = 0.2511$, and muon fluxes from neutralino annihilations in the Sun and Earth of $\Phi_\mu^\ominus = 143.3$ muons/km²/yr and $\Phi_\mu^\oplus = 44.25$ muons/km²/yr, respectively. In order to examine how the scattering cross section changes with the annihilation cross section, we varied the higgsino and gaugino mass parameters of the original model, μ and M_2 , while keeping the neutralino mass and all the other MSSM parameters fixed. This variation produces a “line” in the model parameter space with constant neutralino mass but varying μ and M_2 parameters, and hence different gaugino and higgsino compositions. Fig. 1 shows plots of the spin-independent neutralino-proton scattering cross section $\sigma_{\chi-p}$, the neutralino-neutralino annihilation cross-section at zero temperature and momentum $\langle\sigma_a v\rangle$, and the neutralino relic density $\Omega_\chi h^2$, all plotted versus $Z_g/Z_h = Z_g/(1 - Z_g)$, the ratio of gaugino and higgsino fractions (defined such that $Z_g + Z_h = 1$). The range of μ and M_2 used to produce Fig. 1 was $150 \text{ GeV} < \mu < 1.2 \text{ TeV}$ and $8.9 \text{ TeV} > M_2 > 290 \text{ GeV}$.

From the plot we see that for mixed and gaugino-like neutralinos ($Z_g > 0.1Z_h$) there is an excellent correspondence between $\Omega_\chi h^2$ and $\langle\sigma_a v\rangle$: as the annihilation cross section in the Earth or Sun increases, the relic density decreases and vice-versa, as expected. Furthermore, we see evidence of the crossing symmetry at work by examining the scattering and annihilation cross sections: as the annihilation cross section increases, so does the scattering cross section.

This correspondence makes neutralino models with low relic densities but large direct and indirect detection rates possible. Fig. 1 shows that the crossing symmetry is not effective when the neutralino has a small gaugino component ($Z_g < 0.1Z_h$). One reason the crossing symmetry is not perfect at low Z_g is because annihilation into W and Z pairs dominates for these neutralinos. Hence, the annihilation cross section remains large, but the scattering cross section decreases at low Z_g . Moreover, at low Z_g , the neutralino is almost a pure higgsino and is almost degenerate in mass with the second lightest neutralino and the lightest chargino. Therefore, coannihilations between neutralinos and charginos make $\langle\sigma_a v\rangle_{E,U}$ larger than $\langle\sigma_a v\rangle$. In fact, taking coannihilations out, we find that the neutralino density without coannihilations, shown in Fig. 1 with the line labelled “w/o coanns”, would be inversely proportional to $\langle\sigma_a v\rangle$.

In the rest of this paper, we study the concrete case of the lightest neutralino. For this purpose, we use a table of models allowed by all accelerator limits (but without imposing any constraint from the recent measurement of the muon anomalous magnetic moment [8]). The table has been produced with the DarkSUSY code [7] over the last few years for other purposes, i.e. having in mind other issues which were addressed in the papers of Ref. [6, 9] for which the models were originally computed. Thus, to produce all the remaining figures, we have not done any particular sampling of the models to favor lower densities and higher detection rates. We restricted our attention to models with $\Omega_\chi \leq \Omega_{DM} = 0.3$ ($\Omega_\chi h^2 \leq 0.15$) for which we found about 45,000 points in parameter space.

We use this table of models to show the validity of Eq. (2). In Fig. 2 we plot $\Omega_\chi h^2$ versus the zero momentum (and zero temperature) limit of the neutralino-neutralino annihilation cross section times relative velocity $\langle\sigma_a v\rangle$, together with the approximate relation in Eq. (2) (straight line). From the plot we see that Eq. (2) is a good approximation for the models with the largest $\langle\sigma_a v\rangle$. Generally, points are to the right and below the line because the cross sections increase with energy and more annihilation channels, including coannihilations, are open in the early universe. Some points are to the left of the line due to resonances active at low energy, or above the line due to coannihilations with particles which have a lower annihilation cross section than neutralinos.

In a previous paper [4], the same table of models was used to study the possibility of direct detection of a subdominant component of neutralinos and it was concluded that many models of subdominant neutralinos, even with WIMP halo fractions as low as 10^{-4} , are within the discovery limit of proposed detectors in the conceivable future.

We now examine indirect detection of a subdominant neutralino component.

A proposed method of indirect detection consists of searching for gamma-rays and rare cosmic rays produced by WIMP annihilations in dark halos [10] or at the galactic center [11]. The rate of these annihilations scales as

$$\Gamma \sim \sigma_a \rho_\chi^2. \quad (3)$$

Since, as discussed above, ρ_χ scales as Ω_χ and σ_a scales approximately as $1/\Omega_\chi$, the annihilation rate in the halo scales approximately as Ω_χ . As an example of halo fluxes, Fig. 3 shows the solar-modulated flux of anti-protons from neutralino annihilations in the halo versus the neutralino relic density, together with the BESS 1- σ measurement [12], both at 1 GeV kinetic energy and solar minimum. The envelope of maximum fluxes decreases linearly, not quadratically, with decreasing density. This shows that even if an increase in the cross section compensates the decrease in one of the powers of the density, fluxes still decrease linearly with the halo WIMP density. Hence WIMPs which are a subdominant component of the total CDM would be extremely difficult to detect through this method, as already concluded in [4, 5]. However, we expect that the intensity of the high-energy neutrino emission from the Sun and the Earth would in many cases remain high with decreasing density.

As the Sun and Earth orbit about the center of the galaxy, they sweep through the dark matter halo. Interactions with nuclei within the Sun and Earth slow WIMPs enough such that the WIMPs can become gravitationally captured. The WIMP capture rate of a macroscopic body is given by [13]

$$C = \pi \frac{\rho_\chi}{m_\chi} F(0) \sum_i \frac{(\sigma_{\chi-i})_s}{m_i} \beta_i M \langle v_{e,i}^2 \rangle \langle v_{cut,i}^2 \rangle \sim \langle \sigma_s \rangle \rho_\chi, \quad (4)$$

where ρ_χ is the halo density of the WIMPs, m_χ is the mass of the particular WIMP, $(\sigma_{\chi-i})_s$ is the elastic scattering cross section of the WIMP with the i -th type of nucleus in the body, β_i is the fraction of the body's mass in that nucleus, M is the total mass of the body, $\langle v_{e,i}^2 \rangle$ is the squared escape velocity and $\langle v_{cut,i}^2 \rangle$ is the squared speed at which capture is kinematically cutoff, both averaged over the mass distribution of the i -th element. $F(0)$ is the zero-velocity phase space distribution of the WIMPs and we call $\langle \sigma_s \rangle$ the averaged scattering cross section appearing in the capture rate C . Furthermore, the annihilation rate Γ_A of captured WIMPs within the body can be written in terms of the capture rate as [14]

$$\Gamma_A = \frac{C}{2} \tanh^2 \left(\frac{t}{\tau_A} \right) \quad (5)$$

where t is the age of the body and $\tau_A = (CC_A)^{-1/2}$ is the equilibration time between capture and annihilation. C_A , the annihilation rate per WIMP pair, can be written in terms of effective volumes V_1 and V_2 as $C_A = \langle \sigma v \rangle_A V_2/V_1^2$, where the effective volumes depend on the pressure and temperature within the body in question ($V_j = 3T_0/(2jm_\chi G\rho_0)$, where T_0 and ρ_0 are the core temperature and density of the Sun or Earth).

When the equilibration time is much shorter than the age of the body, $\tau_A \ll t$, the WIMP population is in equilibrium, i.e. the annihilation rate and the capture rate are equal (apart from a factor of two). In this case,

$$\Gamma_A \simeq \frac{C}{2} \sim \langle \sigma_s \rangle \rho_\chi. \quad (6)$$

If a decrease in WIMP relic density is compensated by a corresponding increase in the scattering cross section, the annihilation signals from Sun and Earth remain constant as the relic density decreases.

If instead the equilibration time is much longer than the age of the body, $\tau_A \gg t$, then

$$\Gamma_A \simeq \frac{C}{2} \left(\frac{t}{\tau_A} \right)^2 \simeq C_A C^2 t^2 \sim \langle \sigma_a v \rangle \langle \sigma_s \rangle^2 \rho_\chi^2 \sim \langle \sigma_a v \rangle \frac{\langle \sigma_s \rangle^2}{\langle \sigma_a v \rangle_{E.U.}^2}. \quad (7)$$

Thus if the scattering cross section rises as the annihilation cross section increases to decrease the current density of neutralinos, the annihilation rate may remain high. In this regime, overcompensation, namely a rise in the neutrino flux despite decreasing relic neutralino densities, is possible. Namely, if $\langle \sigma_s \rangle / \langle \sigma_a v \rangle_{E.U.}$ is constant, then $\Gamma_A \sim \langle \sigma_a v \rangle \sim \langle \sigma_a v \rangle_{E.U.} \sim \Omega_\chi^{-1}$. This overcompensation is different from the increase in rates in direct and indirect detection qualitatively put forward in Ref. [5] (see Fig. 2 in the first paper of Ref. [5]), which for indirect detection would hold in the case of equilibrium between capture and annihilation. Ref. [5] stated that rates either remain constant or increase slightly with decreasing densities. Below we see that this statement holds only at relatively high subdominant relic densities, while for smaller densities rates decrease (see Fig. 5 below for indirect detection, and Fig. 2 in Ref. [4] for direct detection).

Notice that $\tau_A = (CC_A)^{-1/2}$ is

$$\tau_A \sim \left(\langle \sigma_s \rangle \frac{\langle \sigma_a v \rangle}{\langle \sigma_a v \rangle_{E.U.}} \right)^{-1/2}. \quad (8)$$

Thus, if both $\langle \sigma_a v \rangle$ and $\langle \sigma_a v \rangle_{E.U.}$ increase about equally, then $\tau_A \sim \langle \sigma_s \rangle^{-1/2}$. Hence a smaller τ_A corresponds to a larger scattering cross section. Since capture is more efficient for large $\langle \sigma_s \rangle$, the highest fluxes will come from the models with the smallest τ_A .

Figs. 4a and 4b illustrate this clearly¹. There we plot the muon rates in underwater or under-ice detectors (such as AMANDA [15], IceCube [16], ANTARES [17], and NESTOR [18]) from annihilation in the Sun and the Earth as functions of the equilibration time τ_A . (The vertical dashed line in figs. 3a and 3b denotes the age of the solar system, 1.5×10^{17} s.) These muons are produced by the neutrinos generated in neutralino annihilations in the Earth or the Sun. These neutrinos interact with matter in or near the underwater or under-ice detectors through the charged current interaction $\nu N \rightarrow \mu X$ producing muons. In this paper, we take the energy threshold of detectable muons to

¹Notice that while in the other figures we use a regular grid of points covering the region with models, in Figs. 4, 7, 8 and 9c, d and e below we show the original points in the table of models. No meaning should be assigned to the density of points, as the latter is an artifact of the scanning used to generate the table of models (see discussion in Ref. [6]).

be 25 GeV, which is a reasonable value for IceCube, and assume that it will be possible to detect a flux of 10 upward-going muons/km²/yr.

For the Sun (Fig. 4a), τ_A can be $\ll t$, $\simeq t$ or $\gg t$. The highest fluxes correspond to $\tau_A \ll t$, namely to models for which equilibration between capture and annihilation has taken place. So for the Sun, we do not expect overcompensation. In fact, in Fig. 5, which shows the neutrino-induced up-going muon fluxes as a function of the relic density $\Omega_\chi h^2$, we see compensation down to densities of $\Omega_\chi h^2 \simeq 10^{-2}$, and a suppression of the rate for lower densities. In this figure we include all neutralino masses, since the flux of neutrinos from the Sun does not change much with neutralino mass. Present bounds from MACRO [19], Baksan [20], and Super-Kamiokande [21] exclude fluxes higher than approximately 10³ muons/km²/yr. Models with $\Omega_\chi h^2 \simeq 1 \times 10^{-3}$ may have signals above 10 muons/km²/yr. So a kilometer-size detector may be able to probe even neutralinos which constitute only 0.7% of the dark halo using neutrino signals from the Sun.

The Earth is either in the regime where $\tau_A \gg t$ or in the regime in which $\tau_A \simeq t$ (see Fig. 4b). Thus the highest fluxes correspond to $\tau_A \simeq t$. Equilibration between capture and annihilation is not reached, and so we expect cases with overcompensation. In fact, this is apparent in Fig. 6a, where we plot the muon fluxes from neutralino annihilations in the Earth as function of $\Omega_\chi h^2$ for neutralinos lighter than 150 GeV. The envelope of the highest fluxes increases with decreasing densities down to values of $\Omega_\chi h^2 \simeq 3 \times 10^{-3}$. Close to this value of $\Omega_\chi h^2$, which corresponds to a neutralino fraction in the halo of only 2%, the muon fluxes become higher than 10 muons/km²/yr, while signals from the Earth from neutralinos constituting the whole of the halo would only reach the level of 1 event/km²/yr (with a threshold of 25 GeV). With the energy threshold of 25 GeV, neutralinos lighter than 150 GeV are expected to be within reach of a kilometer-size neutrino telescope searching for neutrino signals from the Earth only if they are subdominant.

For neutralinos heavier than 150 GeV, the envelope of the highest muon fluxes from the Earth remains almost constant with decreasing densities down to $\Omega_\chi h^2 \simeq 5 \times 10^{-3}$ (see Fig. 6b). There are expected rates above 10 muons/km²/yr for densities as low as $\Omega_\chi h^2 \simeq 3 \times 10^{-3}$, i.e. a kilometer-size neutrino telescope may detect neutrino signals from the Earth for neutralinos with a halo fraction from 1 to as low as 2%.

The predicted fluxes from the Earth are all below the current upper limits of approximately 10³ muons/km²/yr from MACRO [19], Baksan [20], Super-Kamiokande [21] and AMANDA [22]. Notice that in similar figures appearing in the literature (e.g. in Ref. [22]) there are models with signals higher than shown here. The reason is a lower experimental energy threshold (e.g. 1 GeV) and a different choice of the minimum density value the neutralinos can have to constitute the whole of the halo ($\Omega_\chi h^2 = 0.025$ instead of 0.15).

If detection of a direct or indirect dark matter signal occurs, some model discrimination could be achieved by looking for a signal in other ways. This is

illustrated in Figs. 7a, 7b and 8a, 8b.

In Fig. 7a we present the fluxes of up-going muons produced by neutralino annihilations in the Earth versus relic density, for all models with fluxes from the Sun larger than 10 muons/km²/yr. This figure shows that only some of the models detectable from the Sun are also visible from the Earth. Contrariwise, all the models detectable from the Earth produce signals also detectable from the Sun, as can be seen in Fig. 7b, where we present the fluxes from the Sun of models with fluxes from the Earth above 10 muons/km²/yr, again versus relic density. Notice that the points plotted have densities ranging from 100% to 1% of the halo dark matter density. The big range of fluxes in Fig. 7a is due to the fact that the capture rate in the Sun depends on both the spin-independent and spin-dependent scattering cross sections, while the capture in the Earth only depends on the spin-independent scattering cross section.

The points in Fig. 7b visible from both the Earth and the Sun in kilometer-size neutrino telescopes are also plotted in Fig. 8a, which shows that all of them are within the sensitivity reach of the current generation of direct dark matter detectors (such as CRESST II [23], ZEPLIN II [24], CDMS-Soudan [25], and EDELWEISS II [26]). Fig. 8a presents the spin-independent scattering cross section of neutralinos with protons multiplied by the neutralino halo fraction (the product that enters the direct detection rate) versus the neutralino mass, for models producing fluxes higher than 10 muons/km²/yr from both the Earth and (therefore also) the Sun. In the figure we include the CDMS [27] and EDELWEISS 2000-2002 [28] direct dark matter search limits, as these bounds are currently the most stringent. The CDMS and EDELWEISS 2000-2002 limits, which we have not imposed on the models, eliminate several neutralino models with high fluxes from both the Earth and the Sun. However, many models fall outside the current bounds but within the discovery limit of the current generation of detectors.

Regarding indirect signals from the Sun, on the other hand, not even the larger direct-search detectors of the next generation (such as ZEPLIN IV [24], CryoArray [29], GENIUS [30], and XENON [31]) will be able to examine all models that give a detectable signal from the Sun in a kilometer-size neutrino telescope. In fig. 7b, the models producing more than 10 muons/km²/yr from the Sun are plotted in the rescaled spin-independent scattering cross section versus mass plane. Although several models fall within the sensitivity reach of future direct detectors, several others fall outside. The latter are those with small spin-independent cross sections but large spin-dependent cross sections with protons in the Sun.

Independently of indirect signals, direct searches may reach much lower densities. Figs. 9a to 9e show all the models in our table separated in decades of relic density $\Omega_\chi h^2$ or equivalently halo density fraction f_{CDM} . In Fig. 9a neutralinos constitute between 100% and 10% of the halo, in Fig. 9b between 10% and 1%, in Fig. 9c between 1% and 0.1%, in Fig. 9d between 10^{-3} and 10^{-4} and

in Fig. 9e between 10^{-4} and 10^{-5} of the halo (the smallest density fraction being 2×10^{-5}). In all these figures we plot the rescaled spin-independent scattering cross section (i.e. the spin-independent scattering cross section of neutralinos with protons multiplied by the neutralino halo fraction, which is the product that enters the direct detection rate) versus mass. We also include the present direct-detection bounds and future sensitivity limits. We clearly see in these figures that current data are probing neutralino halo fractions down to 1% (see Figs. 9a and 9b). In the next few years, data are expected from detectors such as CRESST II [23], ZEPLIN II [24], CDMS at the Soudan mine [25], and EDELWEISS II [28]. These experiments will probe halo fractions as small as 10^{-4} (see Figs. 9a,b,c,d). Further in the future, another generation of detectors, such as ZEPLIN IV [24], CryoArray [29], GENIUS [30], and XENON [31], may be able to reach down to neutralino halo fractions of order 10^{-5} , which are the smallest in our table of models.

In summary, indirect detection rates of neutralinos annihilating in the Sun and the Earth remain above present detection thresholds even for neutralinos constituting only 1% of the halo dark matter. Indirect rates are drastically reduced at lower density fractions. We find one instance in which the detectability is highest around a halo fraction of 1%, namely the case of light neutralinos giving neutrino signals from the Earth. We do not find that the detectability of relic neutralinos using signals from Sun or Earth is usually favored for neutralinos of small $\Omega_\chi h^2$, as was previously stated [5].

Present limits from direct detection experiments probe down to 1% of the halo density, while data expected in the near future will probe down to 10^{-4} and the next generation of detectors may reach 10^{-5} of the halo density (as already discussed in Ref. [4]).

Many neutralino models constituting from 1% to 100% of the dark matter halo are detectable in three ways (direct, indirect from the Sun, indirect from the Earth), some in two, and some in only one. Thus if a signal is found either in direct detection experiments or in indirect searches for neutralino annihilations in the Sun or Earth or in both, the question of which component of dark matter was found, the primary or a sub-dominant one, may remain open. However, if a signal would be seen from annihilation in the halo or in the center of the galaxy, it would strongly point towards neutralinos being the dominant component of the dark halo, since the signal from annihilation in the halo decreases sharply with halo fraction.

Acknowledgments

G.D. and G.F. were supported in part by the U.S. Department of Energy Grant No. DE-FG03-91ER40662, Task C. This research was also supported in part by the National Science Foundation under Grant No. PHY99-07949. J.E. thanks the Swedish Research Council for support.

We thank the Kavli Institute of Theoretical Physics at the University of California, Santa Barbara, where this work was completed. We also thank Ted Baltz, David Cline, Philippe di Stefano, Richard Gaitskell, Richard Schnee, and Han-guo Wang for kindly providing data tables for some of the limit and sensitivity curves of direct detection experiments.

References

- [1] D. N. Spergel and P. J. Steinhardt, *Phys. Rev. Lett.* **84**, 3760 (2000).
- [2] K. Griest and D. Seckel, *Phys. Rev. D* **43**, 3191 (1991); J. Edsjö and P. Gondolo, *Phys. Rev.* **D56**, 1879 (1997)
- [3] See, for example, T. K. Gaisser, G. Steigman and S. Tilav, *Phys. Rev. D* **34**, 2206 (1986); B. Sadoulet, in Proc. of the “13th Texas Symposium on Relativistic Astrophysics”, Chicago, Illinois, Dec. 1986, p. 260; K. Griest and B. Sadoulet, in Proc. of the “Second Particle Astrophysics School on Dark Matter”, Erice, Italy, 1988; G. Gelmini, E. Roulet and P. Gondolo, *Nucl. Phys. Proc. Suppl.* **14B**, 251 (1990) and *Phys. B* **351**, 623 (1991); A. Bottino et al., *Astropart. Phys.* **2**, 77 (1994); F. Halzen, in “Int. Symp. on Particle Theory and Phenomenology”, Ames, Iowa, May 1995, astro-ph/9508020 (1995); P. Gondolo, in XXXI Rencontre de Moriond “Dark Matter in Cosmology, Quantum Measurements, Experimental Gravitation”, Les Arcs, France, January 1996, astro-ph/9605290 (1996); V. Berezhinsky et al. *Astropart. Phys.* **5**, 1 (1996); L. Bergström and P. Gondolo, *Astropart. Phys.* **5**, 183 (1996); A. Bottino, F. Donato, N. Fornengo and S. Scopel, *Astropart. Phys.* **13**, 215 (2000) and *Phys. Rev. D* **63**, 125003 (2001).
- [4] G. Duda, G. Gelmini and P. Gondolo, *Phys. Lett. B* **529**, 187 (2002) [hep-ph/0102200].
- [5] A. Bottino, N. Fornengo, S. Scopel, F. Donato, in Results and perspectives in particle physics, La Thuile, 2001 [hep-ph/0105233]; A. Bottino, N. Fornengo, S. Scopel, in COSMO-01, Rovaniemi, Finland, 2001 [hep-ph/0112238]; S. Scopel, *Nucl. Phys. B (Proc. Suppl.)* **110**, 76 (2002).
- [6] L. Bergström and P. Gondolo, *Astropart. Phys.* **5**, 183 (1996).
- [7] P. Gondolo, J. Edsjö, L. Bergström, P. Ullio, and E.A. Baltz, astro-ph/0012234 (2000); <http://www.physto.se/~edsjo/darksusy>.
- [8] H. N. Brown *et al.*, *Phys. Rev. Lett.* **86**, 2227 (2001); G. W. Bennett *et al.*, hep-ex/0208001.
- [9] L. Bergström and P. Gondolo, *Astropart. Phys.* **5**, 183 (1996); J. Edsjö and P. Gondolo, *Phys. Rev.* **D56**, 1879 (1997); L. Bergström, P. Ullio,

- and J. H. Buckley, *Astropart. Phys.* **9**, 137 (1998); L. Bergström, J. Edsjö, P. Gondolo, *Phys. Rev.* **D58**, 103519 (1998); E.A. Baltz and J. Edsjö, *Phys. Rev.* **D59**, 023511 (1999).
- [10] J. E. Gunn, B. W. Lee, I. Lerche, D. N. Schramm, and G. Steigman, *Ap. J.* **223**, 1015 (1978); F. W. Stecker, *Ap. J.* **223**, 1032 (1978); J. Silk and M. Srednicki, *Phys. Rev. Lett.* **53**, 624 (1984).
- [11] P. Gondolo and J. Silk, *Phys. Rev. Lett.* **83**, 1719 (1999) [astro-ph/9906391] and *Nucl. Phys. Proc. Suppl.* **87**, 87 (2000) [hep-ph/0001070]; P. Gondolo, *Phys. Lett. B* **494**, 181 (2000).
- [12] S. Orito *et al.* [BESS Collaboration], *Phys. Rev. Lett.* **84**, 1078 (2000).
- [13] A. Gould, *Ap. J.* **368**, 610 (1991).
- [14] K. Griest and D. Seckel, *Nucl. Phys.* **B283**, 681 (1987); Erratum: *ibid.* **B296**, 1034 (1988).
- [15] R. Wischnewski [AMANDA Collaboration], *Nucl. Phys. Proc. Suppl.* **110** (2002) 510.
- [16] A. Goldschmidt [IceCube Collaboration], *Nucl. Phys. Proc. Suppl.* **110** (2002) 516.
- [17] T. Montaruli [ANTARES Collaboration], astro-ph/0207531 (2002).
- [18] P. K. Grieder [NESTOR Collaboration], *Nucl. Phys. Proc. Suppl.* **97** (2001) 105.
- [19] M. Ambrosio *et al.*, *Phys. Rev.* **D60**, 082002 (1999).
- [20] M. Boliev *et al.*, *Proc. of Dark Matter in Astro and Particle Physics*, 1997, eds. H. V. Klapdor-Kleingrothaus and Y. Ramachers (World Scientific, Singapore, 1997); O. Suvorova, hep-ph/9911415 (1999).
- [21] S. Desai [Super-Kamiokande Collaboration], in *4th International Symposium on Sources and Detection of Dark Matter in the Universe (DM 2000)*, Marina del Rey, California, 2000; A. Habig [Super-Kamiokande Collaboration], in *Proc. XVII International Cosmic Ray Conference (ICRC)*, Hamburg, Germany, 2001, hep-ex/0106024.
- [22] J. Ahrens *et al.* [AMANDA Collaboration], astro-ph/0202370 (2002).
- [23] M. Bravin *et al.*, *Astropart. Phys.* **12**, 107 (1999); M. Altmann *et al.*, astro-ph/0106314 (2001), as tabulated in Ref. [32].
- [24] H. Wang, private communication.

- [25] R. Schnee, private communication; presented by R. Gaitskell at TAUP 99, Nucl. Phys. B (Proc. Suppl.) 87, 77 (2000).
- [26] O. Martineau, talk at *Dark Matter 2002*, Marina del Rey, as appearing in Ref. [32].
- [27] D. Abrams *et al.* [CDMS Collaboration], astro-ph/0203500 (2002).
- [28] A. Benoit *et al.* [EDELWEISS Collaboration], astro-ph/0206271 (2002).
- [29] R. J. Gaitskell, astro-ph/0106200 (2001).
- [30] H. V. Klapdor-Kleingrothaus, in “Beyond the desert 1997,” Castle Ringberg, Germany, eds. H. V. Klapdor-Kleingrothaus and H. Paes (IOP, Bristol, 1998), p. 485; H. V. Klapdor-Kleingrothaus *et al.*, in “Beyond the desert 1999,” Castle Ringberg, Germany, eds. H. V. Klapdor-Kleingrothaus and I. Krivosheina (IOP, 2000), p. 915.
- [31] E. Aprile *et al.*, in *Proceedings of Xenon 2001*, astro-ph/0207670 (2001), as tabulated in Ref. [32].
- [32] R. Gaitskell and V. Mandic, “SUSY Dark Matter/Interactive Direct Detection Limit Plotter,” <http://dmttools.berkeley.edu/limitplots>.

Figure Captions

- Fig. 1** Spin-independent neutralino-proton scattering cross section $\sigma_{\chi-p}$, zero momentum (and zero temperature) limit of the neutralino-neutralino annihilation cross section times relative velocity $\langle\sigma_a v\rangle$, neutralino relic density $\Omega_\chi h^2$, and $\Omega_\chi h^2$ if coannihilations would not occur (“w/o coanns”), as functions of the gaugino fraction Z_g of the neutralino for a specific “line” of models with fixed neutralino mass and all other MSSM parameters held constant (see text).
- Fig. 2** Neutralino relic density $\Omega_\chi h^2$ versus the inverse of the zero momentum (and zero temperature) limit of the neutralino-neutralino annihilation cross section times relative velocity $\langle\sigma_a v\rangle^{-1}$ together with the approximate relation in Eq. (2) (straight line). A regular grid of points shows the region covered with models.
- Fig. 3** Solar modulated anti-proton flux at 1 GeV kinetic energy at solar minimum (using the force-field approximation as implemented in DarkSUSY) as a function of the neutralino relic density. A regular grid of points shows the region covered with models. The horizontal band shows the BESS 1- σ measurement of the antiproton flux.
- Fig. 4** Flux of muons in underground detectors with $E_\mu > 25$ GeV from neutrinos produced in neutralino annihilations in: (a) the Sun, (b) the Earth, as a function of the equilibration time in the Sun or Earth, respectively. Each point represents an actual model. The dashed line shows the current age of the Solar system, 1.5×10^{17} seconds.
- Fig. 5** Flux of muons in underground detectors with $E_\mu > 25$ from neutrinos produced in neutralino annihilations in the Sun as a function of the neutralino relic density. A regular grid of points shows the region covered with models. Approximate indirect detection current bounds and future sensitivity of a kilometer-size detector are indicated.
- Fig. 6** As Fig. 5, but for neutralino annihilations in the Earth and neutralinos with: (a) masses $m_\chi \leq 150$ GeV, (b) masses $m_\chi > 150$ GeV.
- Fig. 7** Flux of muons in underground detectors from neutrinos from neutralino annihilations in: (a) the Earth, (b) the Sun, as a function of the neutralino relic density, for models which concurrently have muon fluxes from neutralino annihilations in (a) the Sun or (b) the Earth with rates greater than 10 muons/km²/yr. Each point represents an actual model.
- Fig. 8** Spin-independent neutralino-proton cross section times neutralino halo fraction as a function of neutralino mass, for models which (a) have muon fluxes from neutralino annihilations both in the Earth and in the Sun with

rates greater than 10 muons/km²/yr, and (b) have muon fluxes from the Sun with rates greater than 10 muons/km²/yr. Each point represents an actual model. Best direct detection current bounds and selected future sensitivity limits are shown.

Fig. 9 Spin-independent scattering cross section of neutralinos with protons times neutralino halo fraction versus mass, together with present direct detection bounds and future sensitivity limits. Models are separated in decades of halo fraction f_{CDM} : (a) $0.1 < f_{CDM} \leq 1$; (b) $10^{-2} < f_{CDM} \leq 0.1$; (c) $10^{-3} < f_{CDM} \leq 10^{-2}$; (d) $10^{-4} < f_{CDM} \leq 10^{-3}$; (e) $10^{-5} < f_{CDM} \leq 10^{-4}$ (the smallest value we found is $f_{CDM} \simeq 2 \cdot 10^{-5}$). In Figs. 9a and 9b, a regular grid of points show the region covered with models, in the others each point represent an actual model.

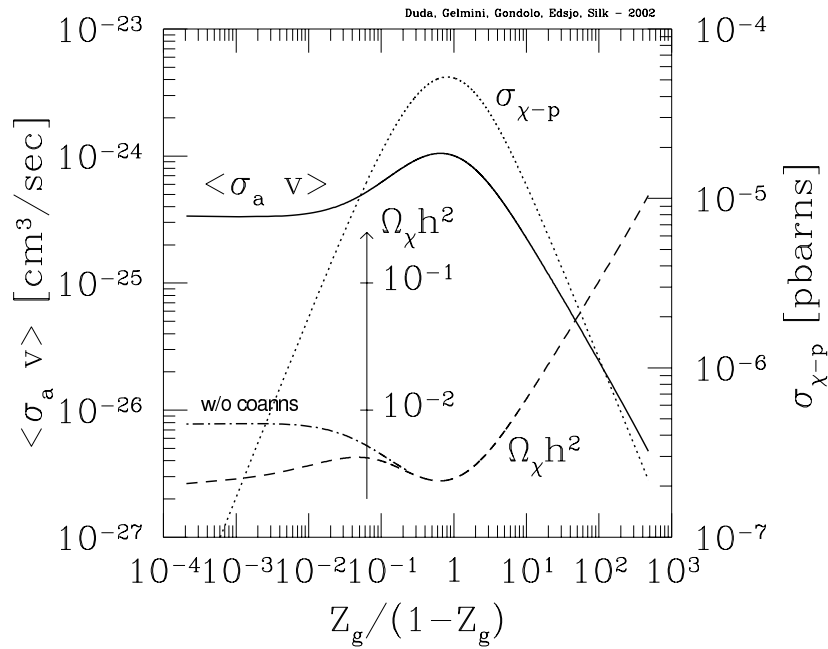


Figure 1.

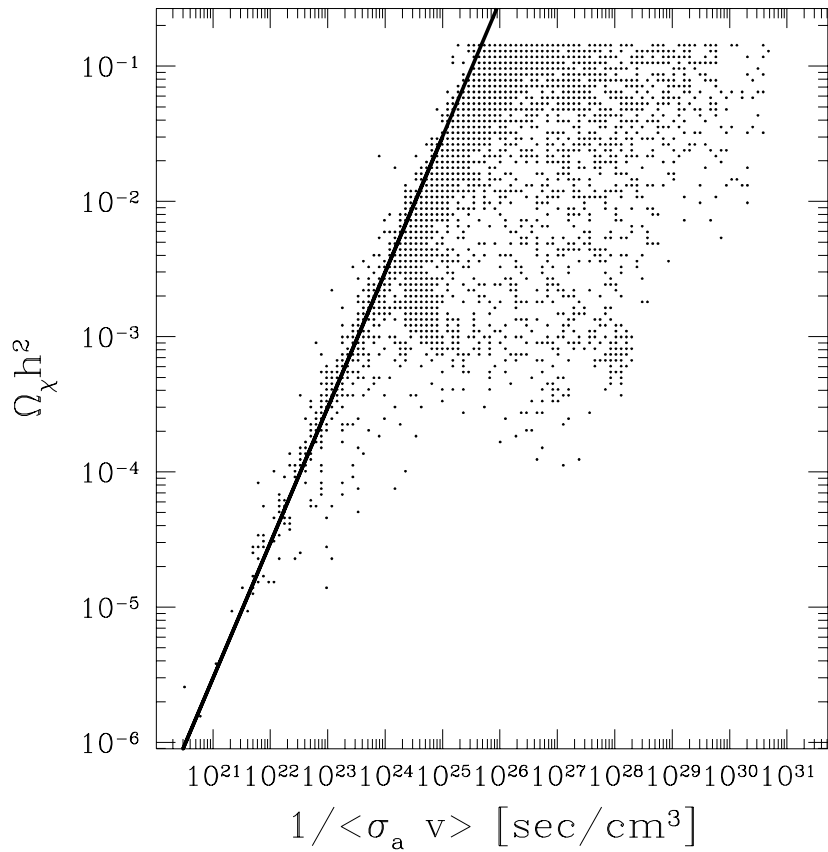


Figure 2.

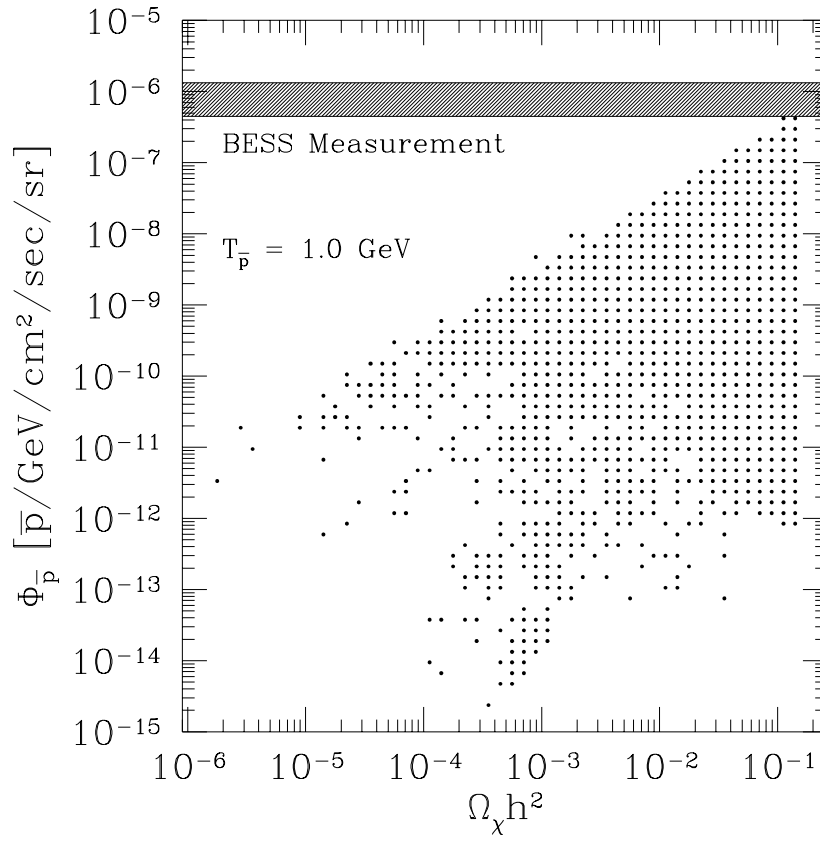


Figure 3.

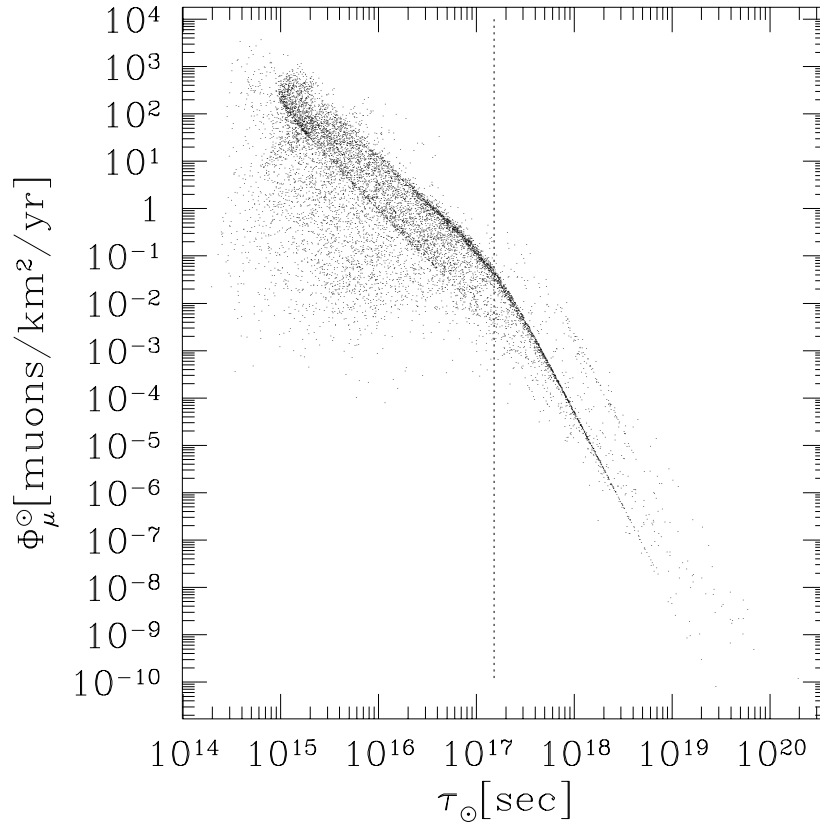


Figure 4a.

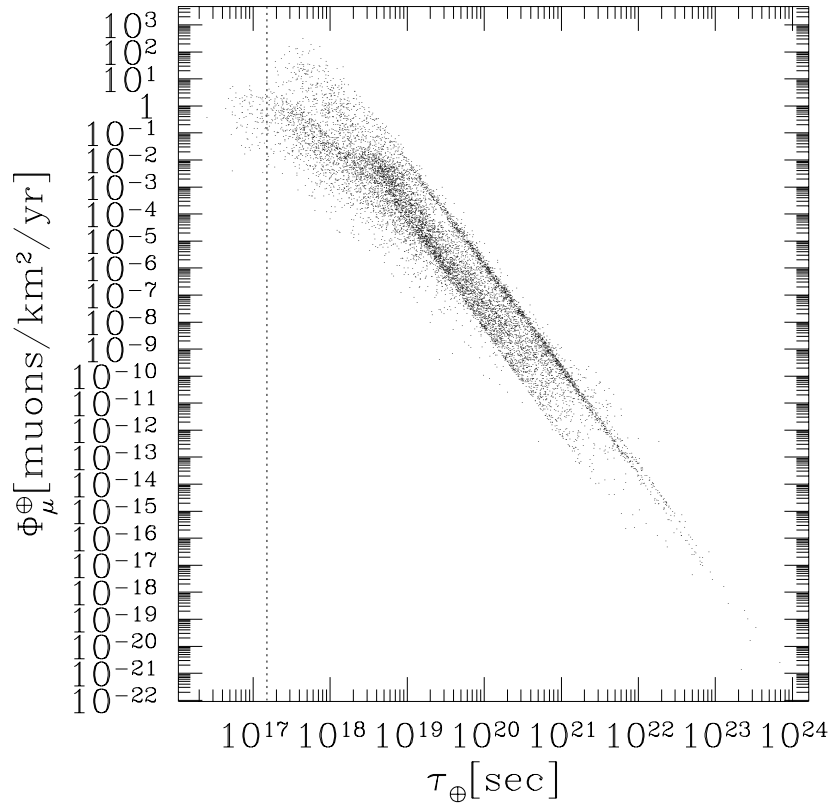


Figure 4b.

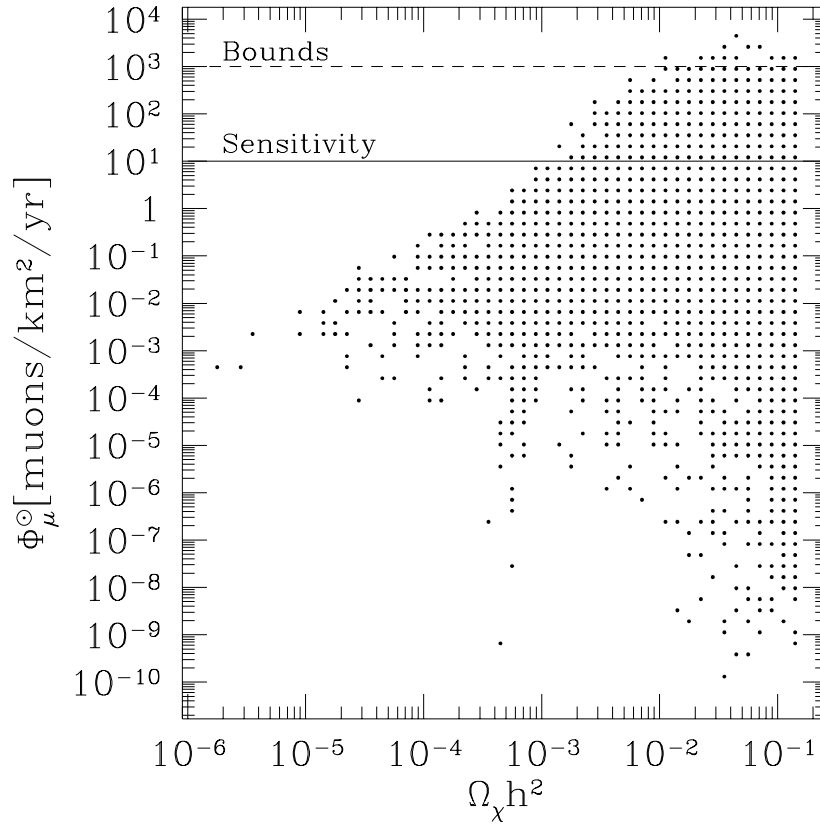


Figure 5.

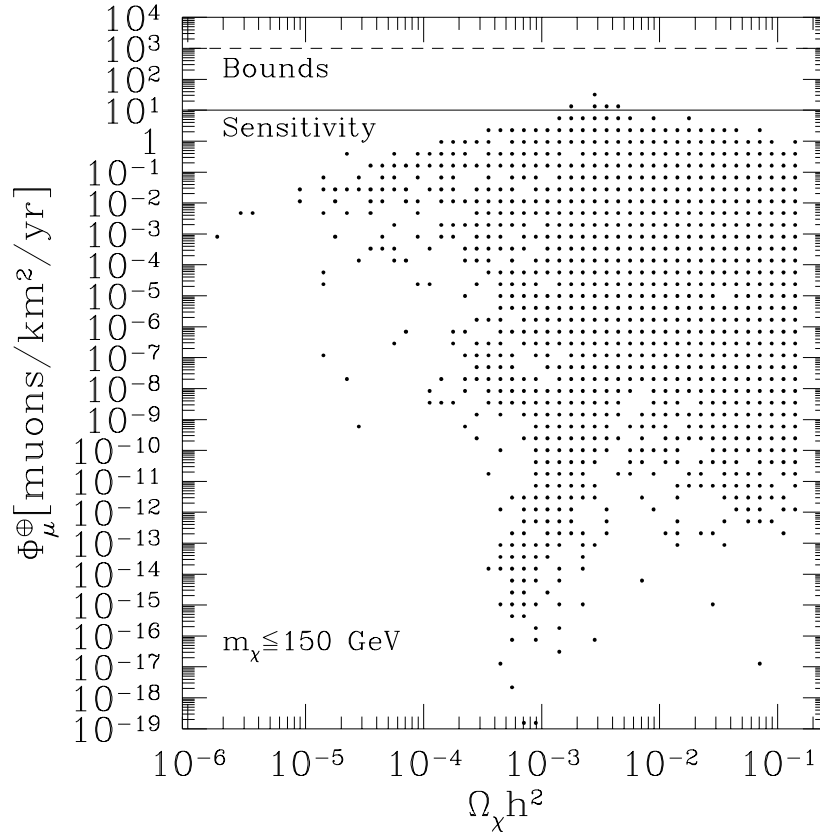


Figure 6a.

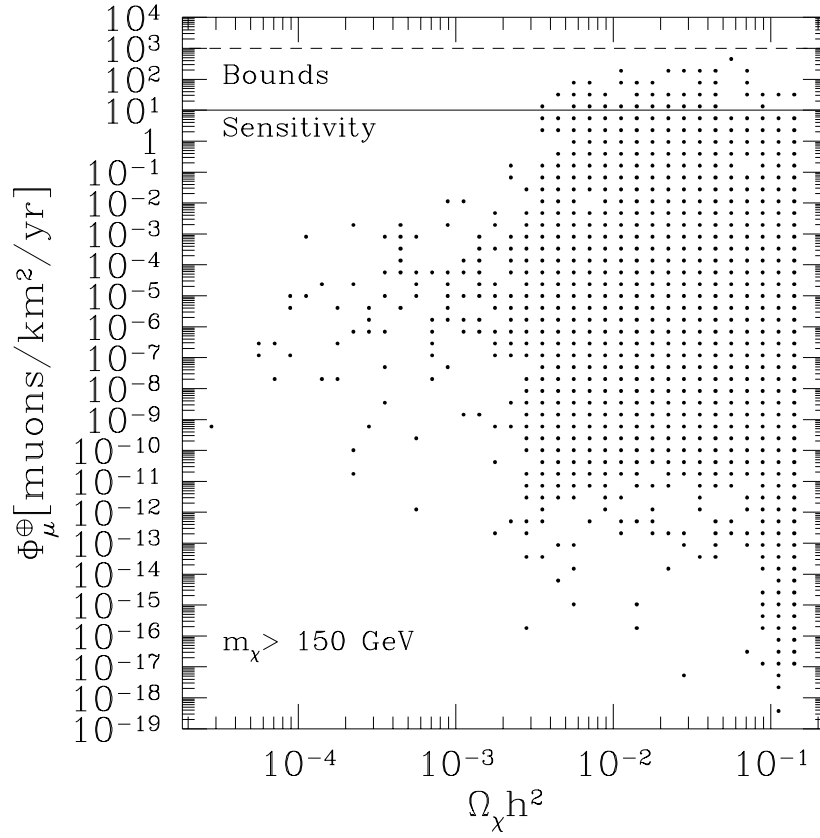


Figure 6b.

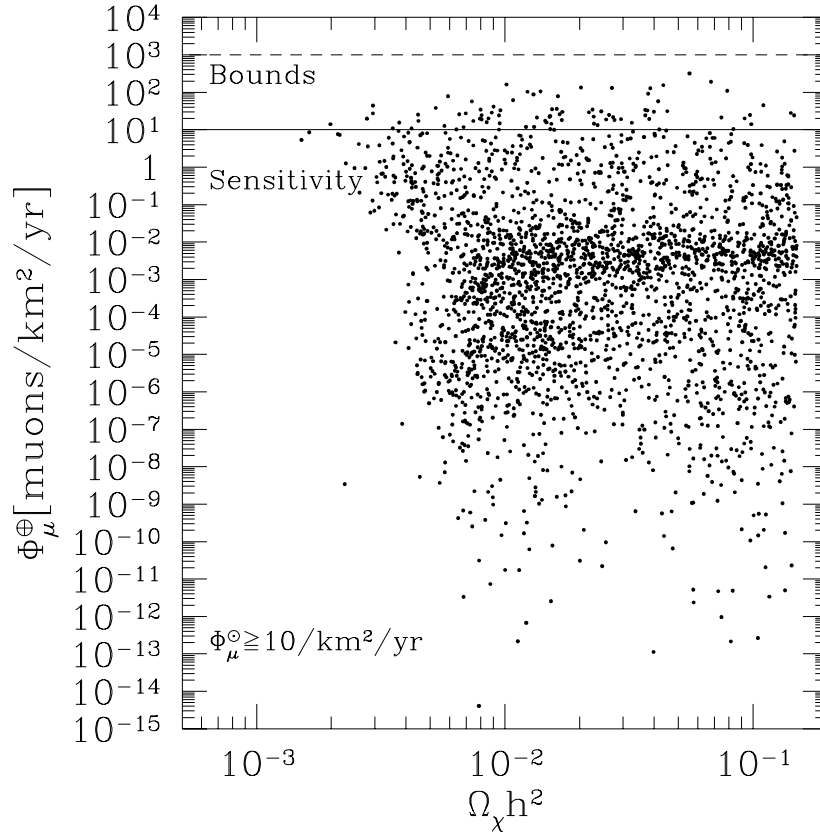


Figure 7a.

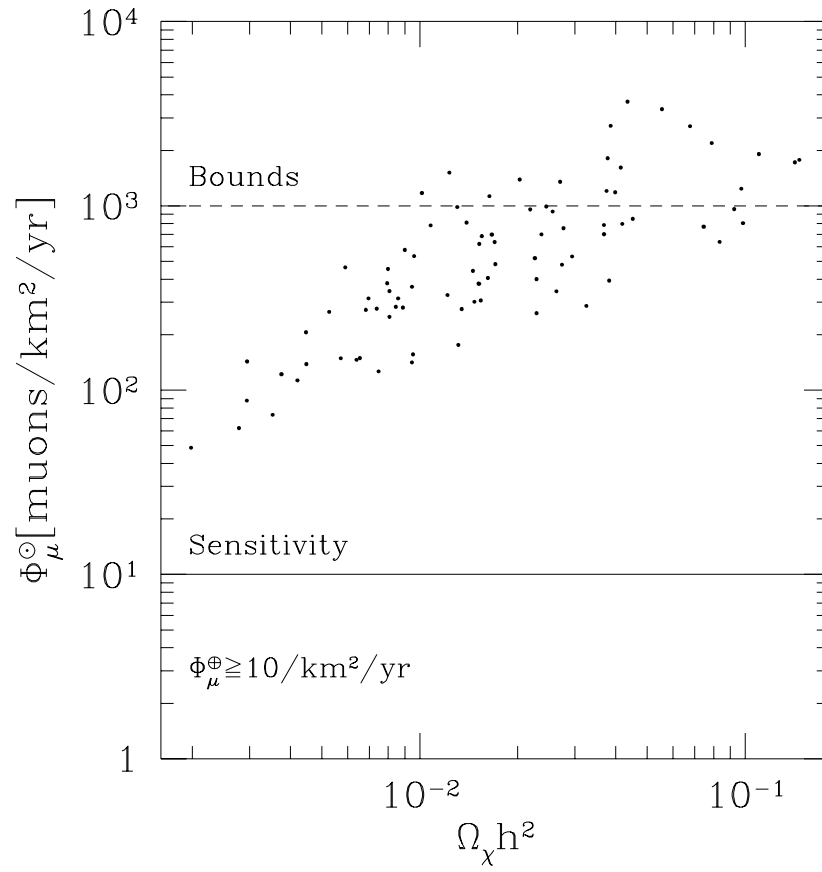


Figure 7b.

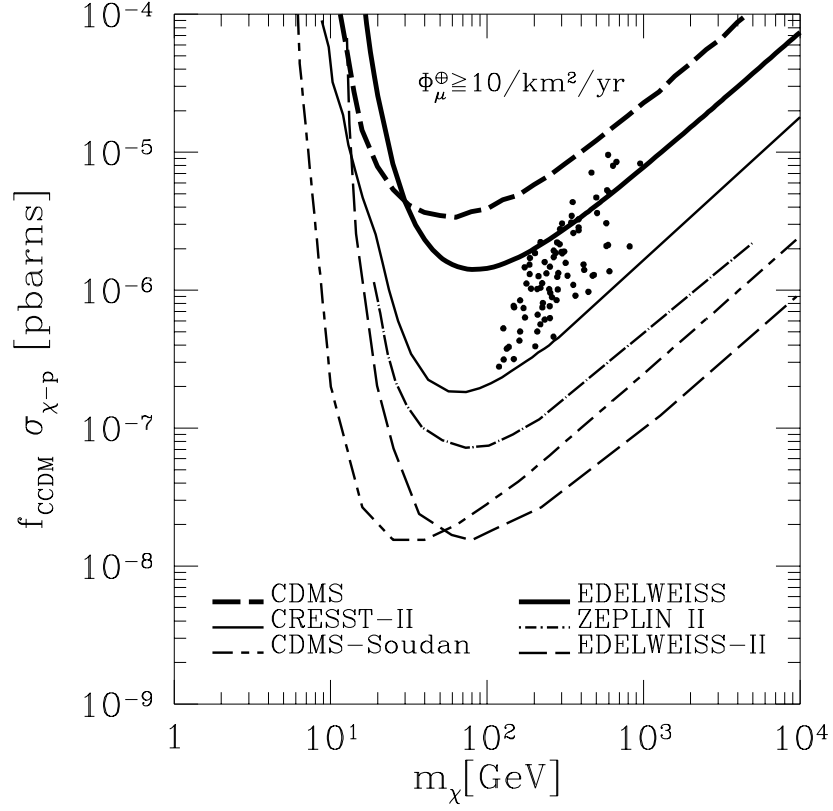


Figure 8a.

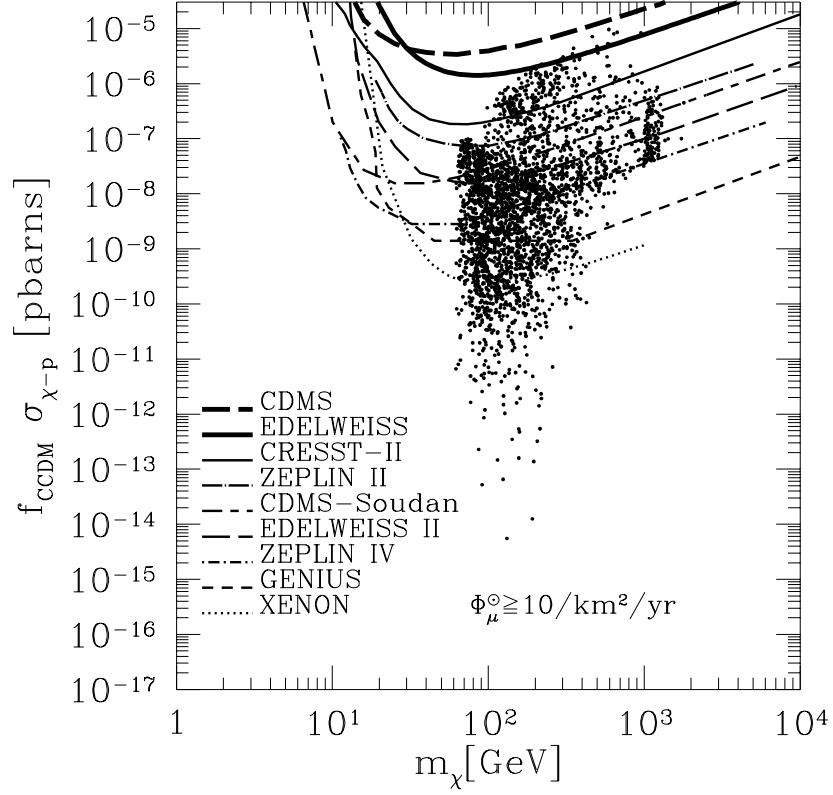


Figure 8b.

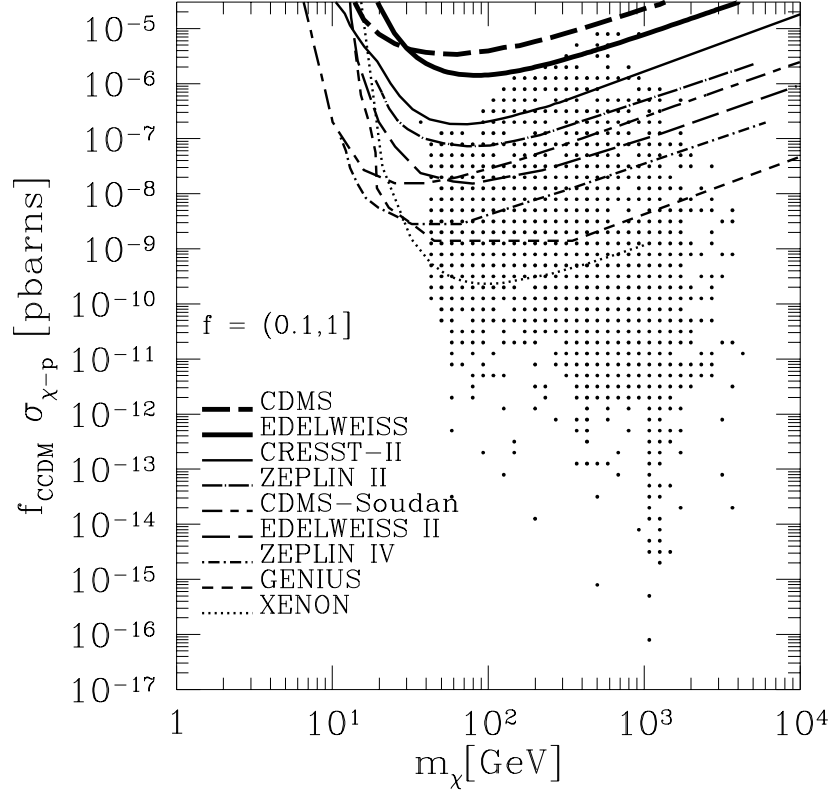


Figure 9a.

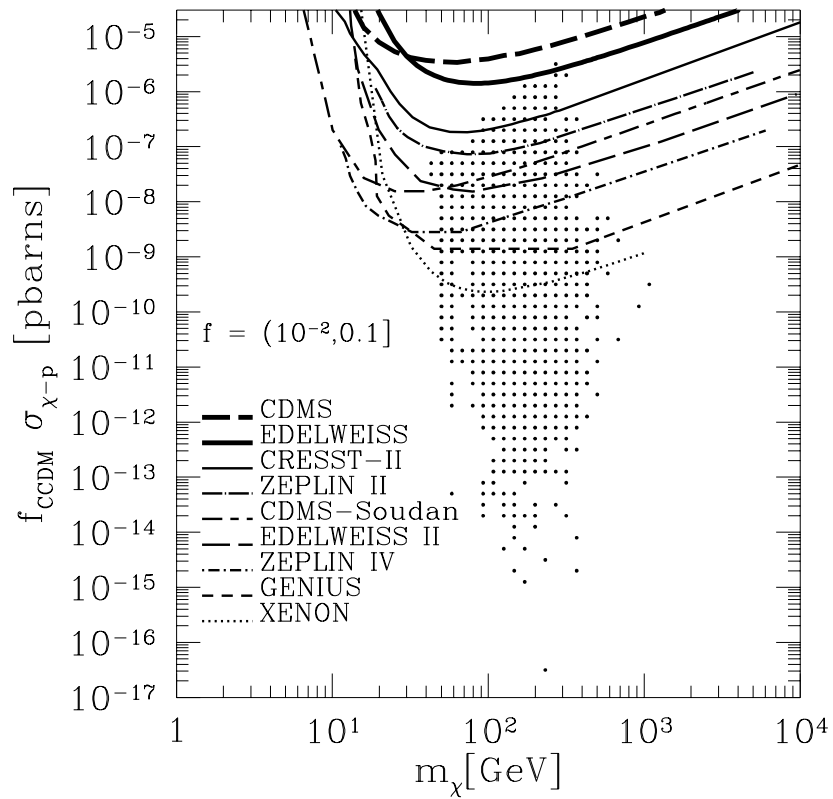


Figure 9b.

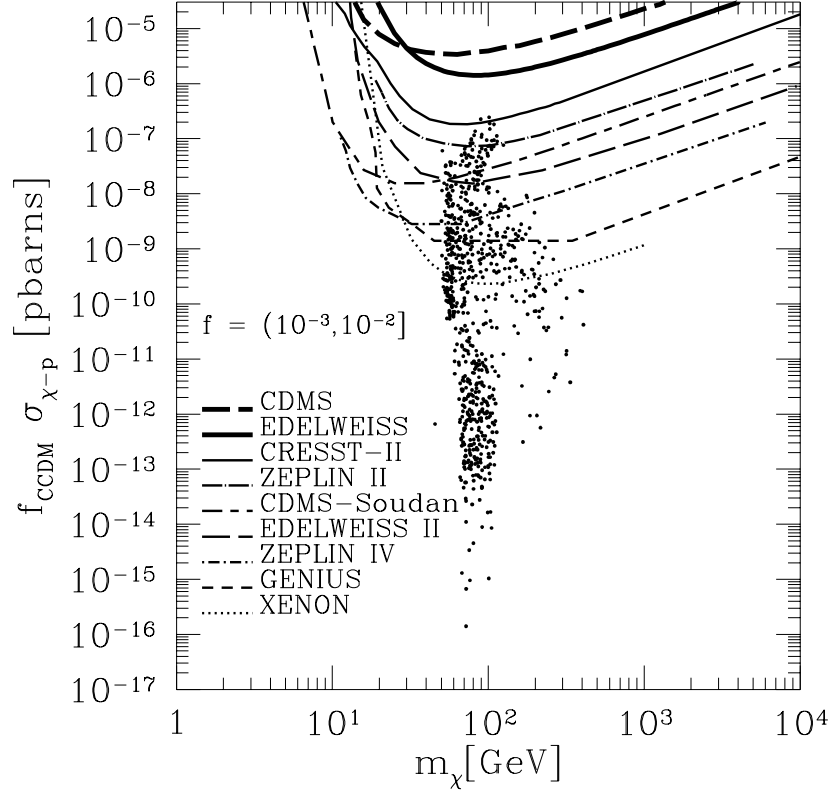


Figure 9c.

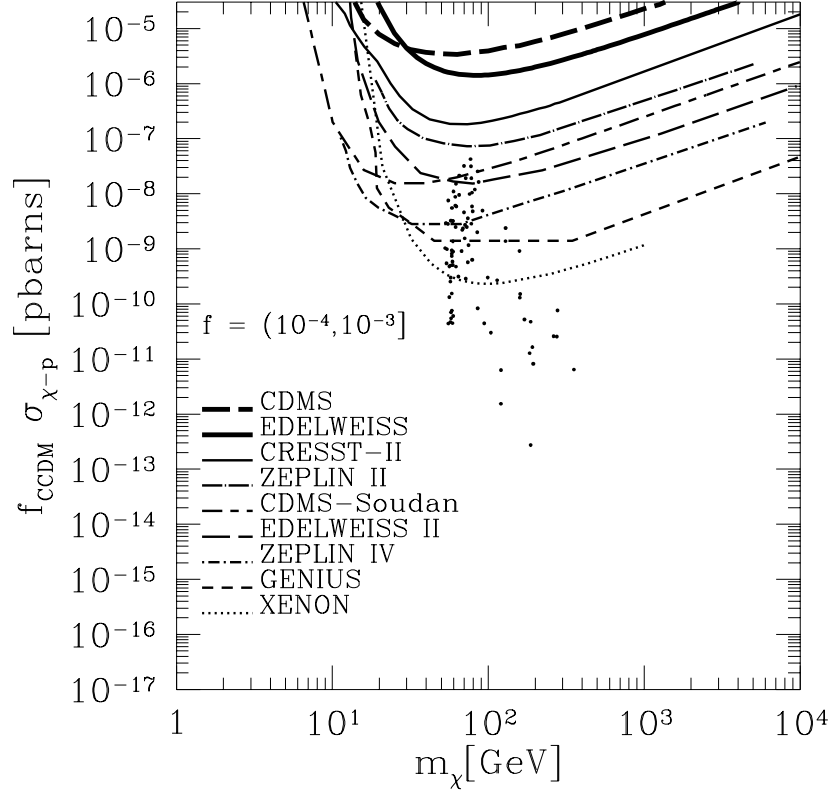


Figure 9d.

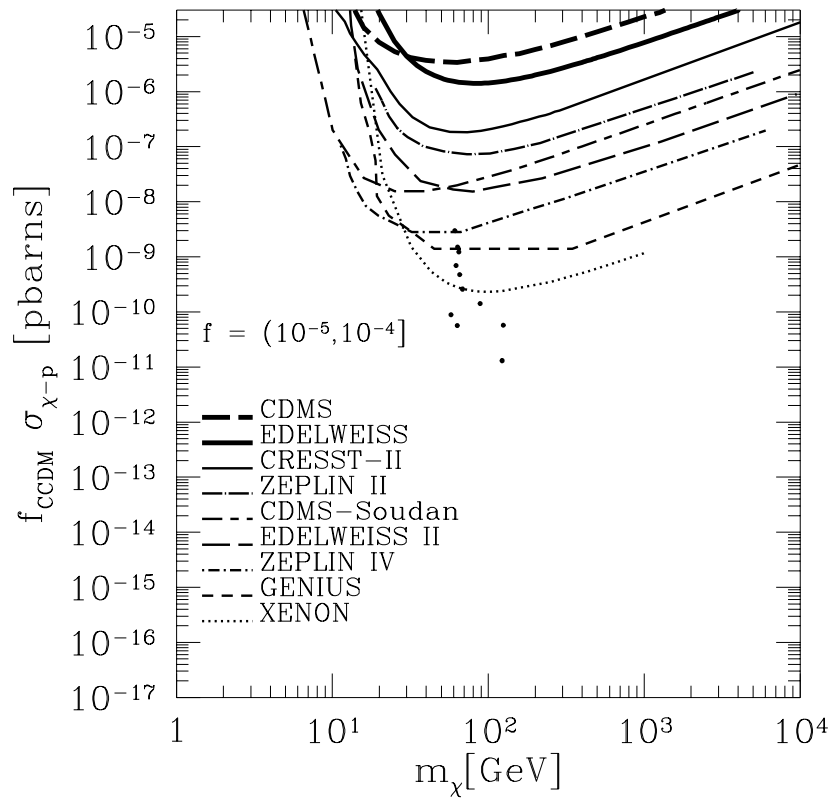


Figure 9e.